Catalysis Letters
https://doi.org/10.1007/s10562-020-03265-1

Copper Iodide Nanoparticles Immobolized Porous Polysulfonamide: An Effective Nanocatalyst for Synthesis of Imidazo [1,2-a] Pyridines

Fatemeh Hamidi Dastjerdi[1] · Ramin Ghorbani-Vaghei[1] · Sedigheh Alavinia[1]

Received: 11 March 2020 / Accepted: 16 May 2020

Abstract

An efficient route was developed for the synthesis of a new polymer, porous cross-linked poly(ethyleneamine)-polysulfonamide (PEA-PSA), as an organic support for the imobilization of CuI nanoparticles (PEA-PSA@CuI). The resulting catalyst works as an efficient recyclable heterogeneous catalyst for the synthesis of imidazo[1,2-*a*] pyridines from the reaction of 2-aminopyridine, aldehydes and phenylacetylene. The method possesses significant advantages including: easy purification, functional group tolerance, recyclability of the catalyst and synthesis of new derivatives in high to excellent yields and short reaction times.

Graphic Abstract

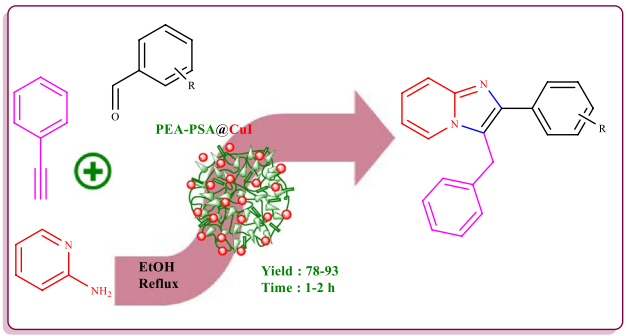

Keywords Porous polysulfonamide · CuI NPs · Heterogeneous · Imidazo[1,2-a]pyridines

1 Introduction

A wide variety of research has been done on cuprous iodide (CuI) due to its distinctive features including: large iconicity and band gap, negative spin–orbit splitting, anomalous diamagnetism behaviour, and unusually large temperature dependency [1, 2]. Potential applications of CuI range from superionic conductors and solid-state solar cells to catalysts for the synthesis of various organic compounds [3]. Besides, various scaffolds have been recently applied in order to assemble and grow copper nanoparticles (Cu-NPs) i.e. Merrifield resin supported phenanthroline copper(I) complex [4], immobilized copper in organic–inorganic hybrid material [5], MCM-41 [6], and glycerol ingrained copper [7]. Owing to the fact that, the organic structure coverage is not a complete one, the NP sized distribution would be broad, and the NPs' spatial arrangement is irregular [8]. As a result developing novel methods for the synthesis of hybrid structures which aim at controlling the mentioned parameters would be highly desirable.

Organic polymers are promising candidates for the matric, due to their ease of processing and handling as compared

Electronic supplementary material The online version of this article (https://doi.org/10.1007/s10562-020-03265-1) contains supplementary material, which is available to authorized users.

✉ Ramin Ghorbani-Vaghei
rgvaghei@yahoo.com

[1] Department of Organic Chemistry, Faculty of Chemistry, Bu-Ali Sina University, 6517838683 Hamadan, Iran

Published online: 28 May 2020

to metals and inorganic glasses [9]. Ligands having sulfonamide groups are excellent in the stabilization of palladium and bromine species [10, 11]. Polysulfonamides are prepared from the reaction between various amines and disulfonyl chloride [10, 11]. In this work, our goal has been to synthesize a novel porous polysulfonamide as a substrate for the stabilization of CuI NPs (PEA-PSA@CuI) [12]. The porousity and coordination interaction between copper and polysulfonamide play an essential role in stabilization of CuNPs. Therefore, we have prepared organic–inorganic nanocomposite materials with CuNPs into a porous polymer matric. The development of porous organic–inorganic nanocomposite with uniform porosity, high loading and a good surface area can provide interesting applications for catalytic reactions [13].

Currently, imidazo[1,2-*a*]pyridine is used in medical applications i.e. cancer, malaria, AIDS treatment etc. [14–17]. During recent years, Gevorgyan et al. reported CuCl-Cu(OTf)$_2$ catalyzed synthesis of imidazo[1,2-*a*] pyridine from a three-component reaction of aldehydes, 2-aminopyridines and terminal alkynes [18]. Moreover, in order to synthesize imidazo[1,2-a] pyridine, various catalysts, i.e. homogeneous [19–22] and heterogeneous catalysts [23–29], have been developed. Accordingly, further research must be done on the environmental impact of the synthesis of imidazo[1,2-*a*] pyridine. Continuing our research [30–34], we aimed at describing an efficient method based on a novel heterogeneous catalyst (PEA-PSA@CuI) (Scheme 1), for the one-pot synthesis of imidazo[1,2-*a*]pyridines (Scheme 2).

2 Experimental

2.1 Reagents and Materials

All materials were purchased from Sigma-Aldrich, Acros and Merck Millipore. Reactions were monitored by thin layer chromatography (TLC) using Merck silica gel 60F254

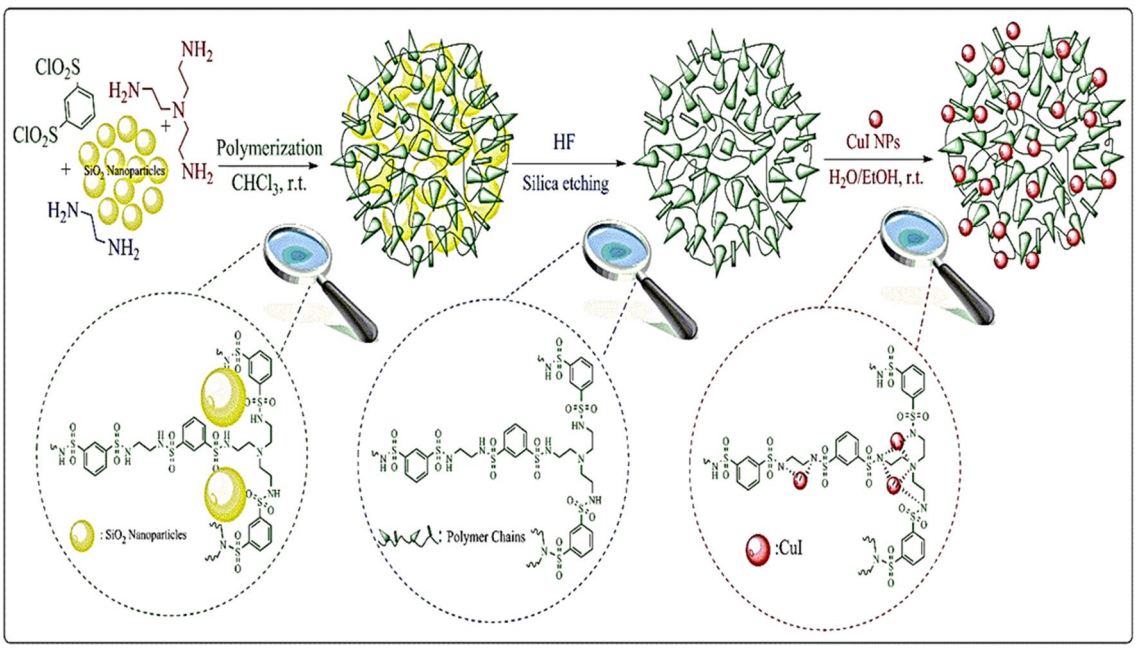

Scheme 1 Total illustration of the synthesis procedure of PEA-PSA@CuI

Scheme 2 PEA-PSA@CuI catalyzed synthesis of imidazo[1,2-a]pyridines

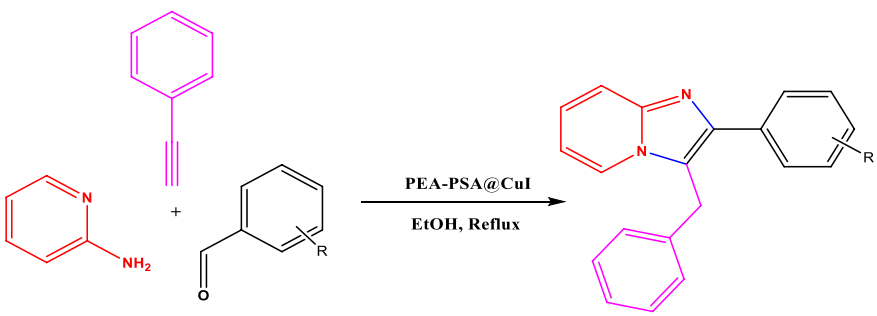

glass plate with 0.25 mm thickness. ^{1}H NMR and ^{13}C NMR spectra were recorded at 400 MHz and 100 MHz, respectively, on a Bruker Avance HD apparatus in $CDCl_3$. Chemical shifts are given on the δ-scale in ppm and residual solvent peaks were used as internal standards.

2.2 General Procedure for the Synthesis of Imidazo[1,2-a]Pyridines

A mixture of 2-aminopyridine (1 mmol) and benzaldehyde (1.1 mmol) was stirred in a 10 mL round bottomed flask. After 5 min, phenylacetylene (1.2 mmol), PEA-PSA@CuI (3.5 mol%, 0.05 g) and EtOH (2 mL) were added and, then, the resulting mixture was stirred under reflux conditions for an appropriate reaction time. Thin-layer chromatography (TLC) was applied to monitor the progress of the reaction. When the reaction was completed, the catalyst was separated by centrifugation. Afterwards, the obtained solid was recrystallized from ethanol in order to give the pure product.

2.3 Analytical Data of the Products

3-Benzyl-2-(4-chlorophenyl)imidazo[1,2-a]pyridine (1a). M.p. 142–144 °C [24]; FT-IR (KBr) ν: 3061, 2926, 1634, 1600, 1487 cm^{-1}; ^{1}H NMR (400 MHz, $CDCl_3$) δ: 4.28 (s, 2H), 6.72 (s, 1H), 6.96 (d, J = 4 Hz, 2H), 7.17–7.24 (m, 5H), 7.42 (s, 1H), 7.53 (s, 2H), 7.61 (s, 1H), 7.97 (d, J = 8 Hz, 1H). ^{13}C NMR (100 MHz, $CDCl_3$) δ: = 29.7, 113.1, 115.0, 125.3, 127.1, 127.5, 127.9, 128.6, 129.1, 129.5, 129.6, 129.9, 130.2, 130.6, 130.9, 131.3, 132.0, 134.0, 136.1. MS: m/z = 318.1[M^+].

3-Benzyl-2-(4-fluorophenyl)imidazo[1,2-a]pyridine (2a). M.p. 84–87 °C [24]; FT-IR (KBr) ν: 3060, 2926, 1657, 1634, 1501 cm^{-1}; ^{1}H NMR (400 MHz, $CDCl_3$) δ: 4.35(s, 2H), 6.81 (s, 1H), 6.92 (s, 1H), 7.02 (s, 2H), 7.29–7.33 (m, 5H), 7.51 (s, 1H), 7.64 (s, 2H), 8.22(s, 1H). ^{13}C NMR (100 MHz, $CDCl_3$) δ: = 30.1, 112.8, 114.8, 114.9, 115.7, 115,8, 124.8, 127.1, 127.8, 127.9, 128.0, 129.1, 129.5, 129.8, 129.9, 131.9, 136.4, 161.3, 163.8. MS: m/z = 319 [M^+].

3-Benzyl-2-(3-nitrophenyl)imidazo[1,2-a]pyridine (3a). M.p. 121–124 °C; FT-IR (KBr) ν: 3065, 2926, 1651, 1627, 1527 cm^{-1}; ^{1}H NMR (400 MHz, $CDCl_3$) δ: 4.40 (s, 2H), 6.76 (t, J = 4 Hz, 1H), 7.03 (d, J = 8 Hz, 2H), 7.19–7.25 (m, 4H), 7.47 (d, J = 4 Hz, 2H), 7.72 (s, 1H), 7.83 (s, 1H),8.09 (d, J = 8, 1H), 8.50 (s, 1H) ppm;^{13}C NMR (100 MHz, $CDCl_3$) δ: = 29.7, 113.5, 115.3, 122.7, 122.9, 127.3, 127.7, 128.0, 128.7, 129.3, 129.4, 132.1, 135.8, 147.9. MS: m/z = 329.36 [M^+].

3-Benzyl-2-phenylimidazo[1,2-a]pyridine (4a). M.p. 118–121 °C [24]; FT-IR (KBr) ν: 3029, 2946, 1635, 1623, 1493 cm^{-1}; ^{1}H NMR (400 MHz, $CDCl_3$) δ: 4.42(s, 2H), 6.79 (t, J = 8 Hz, 1H), 7.08 (d, J = 4 Hz, 2H), 7.29 (d, 8H), 7.73(s, 3H), 8.04 (s, 1H). ^{13}C NMR (100 MHz, $CDCl_3$) δ: = 29.5, 113.2, 118.1, 123.4, 125.3, 127.1, 127.6, 127.9, 128.1, 128.6, 129.1, 133.1, 136.2. MS: m/z = 283.36 [M^+].

3-Benzyl-2-(*p*-tolyl)imidazo[1,2-a]pyridine (5a). M.p. 159–161 °C [24]; FT-IR (KBr) ν: 3026, 2917, 1654, 1627, 1527 cm^{-1}; ^{1}H NMR (400 MHz, $CDCl_3$) δ: 2.31 (s, 3H), 4.41 (s, 2H), 6.79 (t, J = 8 Hz, 1H), 7.10 (d, J = 8 Hz, 2H), 7.16 (m, 2H), 7.28–7.39 (m, 5H), 7.51 (s, 2H), 7.65 (s, 2H) ppm; ^{13}C NMR (100 MHz, $CDCl_3$) δ: = 21.2, 29.8, 112.7, 114.57, 117.0, 123.7, 124.8, 126.9, 128.0, 128.6, 129.7, 131.5, 136.8, 137.9, 142.2, 145.0, 149.7, 152.8. MS: m/z = 298.1[M^+].

3-Benzyl-2-(3-bromophenyl)imidazo[1,2-a]pyridine (6a). M.p. 152–154 °C [24]; FT-IR (KBr) ν: 3060, 2917, 1655, 1631, 1498 cm^{-1}; ^{1}H NMR (400 MHz, $CDCl_3$) δ: 4.39 (s, 2H), 6.81 (t, J = 4 Hz, 1H), 7.07 (d, J = 8 Hz, 2H), 7.12 (s, 1H), 7.29–7.41 (m, 7H), 7.53 (d, J = 12 Hz, 2H), 7.73 (s,1H), 7.83 (s, 1H), 8.20 (s, 1H); ^{13}C NMR (100 MHz, $CDCl_3$) δ: = 29.1, 113.1, 114.9, 123.0, 127.1, 127.9, 128.6, 129.1, 129.3, 130.3, 130.8, 131.2, 132.0, 136.5. MS: m/z = 363.2[M^+].

3-Benzyl-2-(4-methoxyphenyl)imidazo[1,2-a]pyridine (7a). M.p. 129–131 °C [24]; FT-IR (KBr) ν: 3058, 2932, 1633, 1600, 1505 cm^{-1}; ^{1}H NMR (400 MHz, $CDCl_3$) δ: 3.76 (s, 3H), 4.41 (s, 2H), 6.78 (t, J = 8 Hz, 1H), 6.88 (s, 2H), 7.09 (d, J = 8 Hz, 2H), 7.14 (s, 1H), 7.29 (d, J = 4 Hz, 3H), 7.33 (d, J = 8 Hz, 2H), 7.66 (s, 2H), 7.97 (s, 1H), 8.46 (s, 1H); ^{13}C NMR (100 MHz, $CDCl_3$) δ: = 30.1, 55.2, 113.1, 113.7, 115.3, 117.1, 124.9, 127.1, 129.1, 130.3, 131.8, 136.3, 141.7, 149.6, 150.1, 152.5, 159.5, 165.1. MS: m/z = 314.3[M^+].

4-(3-benzylimidazo[1,2-a]pyridin-2-yl)-*N*,*N*-dimethylaniline (9a). M.p. 123–126 °C [25]; FT-IR (KBr) ν: 3072, 2883, 1617, 1600, 1515, 1400 cm^{-1}; ^{1}H NMR (400 MHz, $CDCl_3$) δ: 2.96 (s, 6H), 4.47 (s, 2H), 6.71 (t, J = 4 Hz, 2), 6.75 (s, 1H), 7.15 (d, J = 8 Hz, 2H), 7.24–7.33 (m, 3H), 7.70 (s, 2H); ^{13}C NMR (100 MHz, $CDCl_3$) δ: = 30.1, 40.4, 112.1, 112.3, 123.9, 126.8, 127.7, 128.9, 137.1, 150.1. MS: m/z = 327.43[M^+].

3 Result and Discussion

Through the synthesis of imidazopyridines, the effect of PEA-PSA@CuI as a catalyst was investigated in the synthesis of 3-benzyl-2-phenylimidazo[1,2-*a*]pyridine (4a) as the model compound. At first, we investigated the effect of different amounts of the catalyst on the reaction progress in the model reaction (Table 1, entries 1–3). Results of our studies indicated the formation of the highest yield using 3.5 mol% of the catalyst (Table 1, entry 1). It is worth mentioning

Table 1 Optimization of the reaction conditions in model reaction

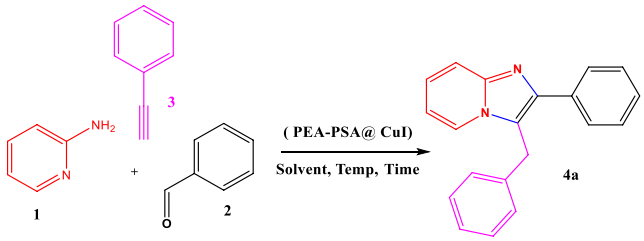

Entry	Catalyst loading	Solvent	Time (h)	Temp. (°C)	Yield (%)[a]
1	PEA-PSA@CuI (3.5 mol %)	EtOH	1.5	Reflux	88
2	PEA-PSA@CuI (7 mol %)	EtOH	1.5	Reflux	89
3	PEA-PSA@CuI (1.7 mol%)	EtOH	4	Reflux	68
4	PEA-PSA@CuI (3.5 mol%)	Solvent-free	5	80	50
5	PEA-PSA@CuI (3.5 mol%)	CH_3CN	5	Reflux	65
6	PEA-PSA@CuI (3.5 mol%)	H_2O	6	Reflux	50
7	PEA-PSA@CuI (3.5 mol%)	EtOH:H_2O (1:1)	6	Reflux	73
8	PEA-PSA@CuI (3.5 mol%)	CH_2Cl_2	6	Reflux	Trace
9	PEA-PSA@CuI (3.5 mol%)	Toluene	6	Reflux	60
10	PEA-PSA@CuI (3.5 mol%)	EtOH	3	r.t	53
11	PEA-PSA@CuI (3.5 mol%)	EtOH	3	50	70
12	PEA-PSA@CuI (3.5 mol%)	Solvent-free	3	100	65
13	PEA-PSA@Ni[b]	EtOH	6	Reflux	Trace
14	PEA-PSA@Pd[b]	EtOH	6	Reflux	34
15	CuCl[b]	EtOH	6	Reflux	22
16	CuBr[b]	EtOH	6	Reflux	30
17	CuI[b]	EtOH	6	Reflux	40
18	CuINPs[b]	EtOH	6	Reflux	55

Reaction conditions: benzaldehyde (1.1 mmol), 2-aminopyridine (1 mmol), phenylacetylene (1.2 mmol), PEA- PSA@CuI (3.5 mol%, 0.05 g), solvent (2 mL)

[a]Isolated yields

[b]Reaction conditions: benzaldehyde (1.1 mmol), 2-aminopyridine (1 mmol), phenylacetylene (1.2 mmol), catalyst, 0.05 g, solvent (2 mL)

that increasing the amount of PEA-PSA@CuI would not affect the reaction progress (Table 1, entry 2). Accordingly, different solvents were applied in order to investigate the catalytic potential of PEA-PSA@CuI i.e. EtOH, H_2O and EtOH:H_2O mixture, dichloromethane, acetonitrile, toluene and solvent-free condition (Table 1, entries 4–9). According to the obtained results, the model reaction was well proceeded with polar solvents including: CH_3CN, EtOH and EtOH:H_2O (1:1). On the contrary, in non-polar solvents, i.e. toluene and dichloromethane, the reaction did not proceed well. When ethanol was applied for the model reaction, a significant increase in the catalytic activity was witnessed with 88% of yield (Table 1, entry 1). When ethanol was used as solvent, more copper nanoparticles were accessible for the catalytic system. Consequently, the catalytic activity was increased. Afterwards, the model reaction was performed at different temperatures (Table 1, entries 10–12). Results demonstrate high catalytic activity in ethanol under reflux condition (Table 1, entry 1). Finally, we examined various catalytic systems including PEA-PSA@Ni (Table 1, entry 13), PEA-PSA@Pd (Table 1, entry 14), CuCl, CuBr, CuI and CuI NPs (Table 1, entries 15–18) comparision to PEA-PSA@CuI (Table 1, entry 1). As can be seen in Table 1, the nanocatalyst exhibited superior behavior in the synthesis of 4a compared with unsupported CuI NPs or other commercial catalyst. The reaction was selective. The starting material are almost consumed and no by-products was observed (based on yield).

With the optimized conditions in hand (Table 1, entry 1), the mentioned conditions' generality to other substrates—applying different electron-withdrawing and electron-donating aromatic aldehydes—were examined. As indicated in Table 2, it is worth mentioning that aromatic aldehydes; containing, –F, –Br, –Cl, $–CH_3$, $–OCH_3$, $–N(CH_3)_2$, and NO_2 groups, were converted to the corresponding product. Benzaldehydes bearing electron-donating

Table 2 Synthesis of imidazo[1,2-a]pyridines using PEA-PSA@CuI

Comp	Aldehyde	Product	Time (min)	Yield (%)[a]
1a	*p*-ClC_6H_4	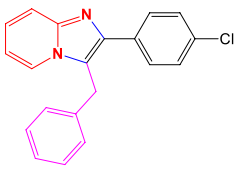	100	85
2a	*p*-FC_6H_4	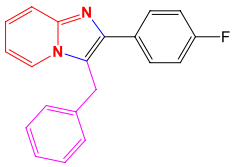	100	90
3a	*m*-$NO_2C_6H_4$	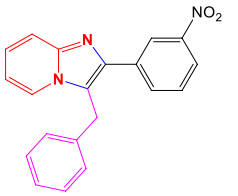	120	78
4a	C_6H_5	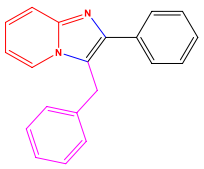	90	88
5a	*p*-MeC_6H_4	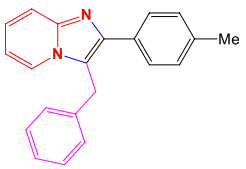	60	80
6a	*m*-BrC_6H_4	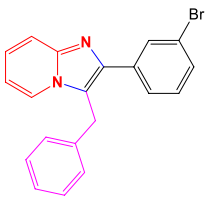	120	87
7a	*p*-$OMeC_6H_4$	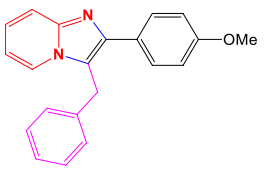	60	93
8a	*o*-ClC_6H_4	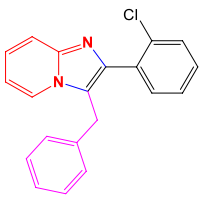	120	83
9a	*p*-$NMe_2C_6H_4$	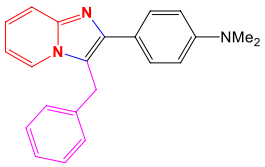	60	90

Table 2 (continued)

Comp	Aldehyde	Product	Time (min)	Yield (%)[a]
10a	p-$NO_2C_6H_4$	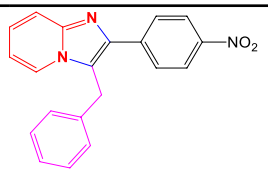	100	92

Reaction conditions: benzaldehyde (1.1 mmol), 2-aminopyridine (1 mmol), phenylacetylene (1.2 mmol), PEA-PSA@CuI (3.5 mol%), solvent (2 mL)

[a]Isolated yields

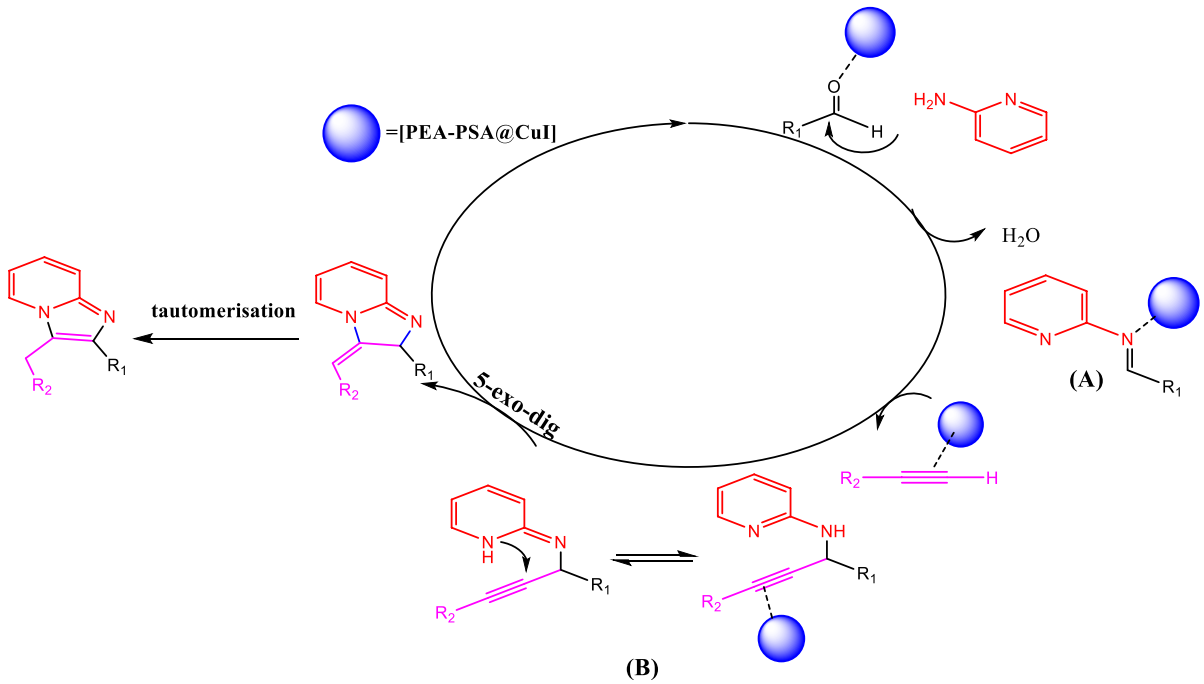

Scheme 3 Suggested mechanism for the synthesis of imidazo[1,2-a]pyridines catalyzed by PEA-PSA@CuI

Table 3 Comparison of the present methodology with other reported catalysts for the synthesis of 3-benzyl-2-phenylimidazo[1,2-*a*]pyridine (4a)

Entry	Catalyst	Condition	Time (h)	Yield (%)	[Refs.]
1	PEA-PSA@CuI (3.5 mol%)	EtOH, reflux	1.30	88, 88, 87, 87, 86, 85	[This work]
2	$InBr_3$ (10 mol%)	Toluene, reflux	12	82	[21]
4	CuI-$NaHSO_4.SiO_2$ (5 mol%)	Toluene, reflux	12	91	[24]
5	Nano-$Fe_3O_4.SiO_2$ (10 mol%)	Toluene, 110 °C	24	89	[25]
6	Cu-nanoparticles (1 mol%)	Solvent-free, 120 °C	12	85	[26]
7	MNP@BiimCu (1.2 mol%)	CTAB, H_2O, reflux	5	90	[27]
8	Nano copper/nano $ZnAl_2O_4$	Solvent-free, 90 °C	6	90	[28]
9	CuO/rGO (0.015 g)	DMSO, 110 °C	6 h	91	[29]

and electron-withdrawing substituents gave the desired products in good to excellent yield. All products were characterized on the basis of their spectroscopic data such as FT-IR, ^1H and ^{13}C NMR spectra and Mass.

The efficiency of PEA-PSA@CuI for the synthesis of 3-benzyl-2-phenylimidazo[1,2-*a*]pyridine (4a) was compared to some other related reports (Table 3). In the present work, using PEA-PSA@CuI as a recyclable catalyst can remarkably enhance the product yield and shorten the reaction time.

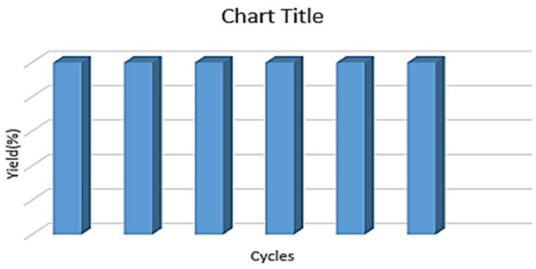

Fig. 1 Recycling of the PEA-PSA@CuI for 3-benzyl-2-phenylimidazo[1,2-a]pyridine (4a)

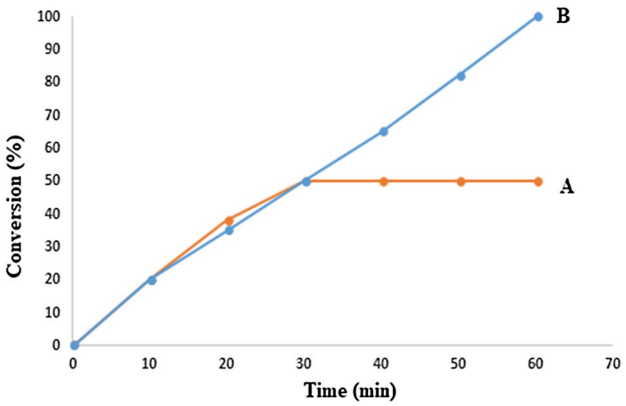

Fig. 2 Hot-filtration test for PEA-PSA@CuI in the reaction of 4-methoxybenzaldehyde, 2-aminopyridine and phenylacetylene, a hot filtered test, b normal reaction

Scheme 3 illustrates a plausible mechanism for the novel catalyst. As regenerated at the end of the cycle, PEA-PSA@CuI appears to be an active catalytic species. As a point of fact, the formation of iminium from the activated aldehyde and 2-aminopyridine can be regarded as the initial event. First, in order to afford the intermediate A, PEA-PSA@CuI which activates aldehyde is followed by nucleophilic addition of 2-aminopyridine. Subsequently, the catalyst would be effective in activating the imine **A.** Moreover, in order to form intermediate B, the phenyl acetylene should react with the intermediate imine **A**. Consequently, we came to this understanding that in order to reach the final product, cyclization and aromatization of the intermediate **B** are necessarily needed [23–29].

In the next step, PEA-PSA@CuI recyclability was evaluated in the model reaction (Fig. 1). Results indicated that the catalyst was successfully recovered and reused for six consecutive runs with a small decrease in the activity (88, 88, 87, 87, 86, 85, respectively). When the reaction was completed, the catalyst was recovered by washing with H_2O/EtOH and dried at 50–60 °C in an oven.

The filtration test for the reaction between 4-methoxybenzaldehyde, 2-aminopyridine and phenylacetylene using PEA-PSA@CuI as a catalyst was performed to check the leaching of CuI NPs during the reaction. A catalytic run was started as for a standard reaction, and after reaction for 30 min (the reaction was completed in 60 min), corresponding to 50% conversion, the reaction mixture was stopped and centrifuged to afford a clear filtrate. Then the mixture without the solid catalyst was treated as a standard catalytic run for another 30 min, and the conversion did not proceed significantly. The results were compared with that of a standard catalytic run. Figure 2 clearly shows that after removal of the heterogeneous catalyst, slow progression of the reaction was observed. This proposes that the prepared catalyst is stable and the leaching of CuI NPs species from the solid support is low.

The recyclability of PEA-PSA@CuI as the catalyst was investigated in the synthesis of 3-benzyl-2-phenylimidazo[1,2-*a*]pyridine (4a) as the model compound. After 5 times, as the FT-IR spectra and Fe-SEM show, the structure of the catalyst didn't significantly change (Figs. 3, 4).

The typical FT-IR spectra of SiO_2/PEA-PSA (a), porous PEA-PSA (b), and PEA-PSA@CuI (c) are shown in Fig. 5. The characteristic peak of SiO_2 at 1112 cm^{-1} is ascribed to Si–O stretching vibrations of silica nanoparticles trapped in polymer chains [35]. This peak does not appear in the FT-IR spectra of the PEA-PSA and CuI@PEA-PSA (Fig. 5b, c). In the spectrum of PEA-PSA, the absorption bands at 1334 and 1163 cm^{-1} are indexed to the S=O stretching vibrations (Fig. 5b). After the coordination of CuI nanoparticles to these situations, the S=O bonds shifted to lower wavenumber (i.e., 1327 and 1152 cm^{-1}) in the spectrum of the final product (Fig. 5c). As can be inferred from these changes, the metal ions are coordinated with the oxygen donor atoms of the PEA-PSA as a ligand. The FT-IR analysis of recycled catalyst showed the stability of the PEAPSA@CuI during the recycling procedure (Fig. 6).

4 Conclusion

In conclusion, we used porous polymer for stabilization of CuI NPs. Using this nanocomposite as a heterogeneous and recyclable catalyst, variety of aldehydes were converted to imidazo[1,2-*a*]pyridines in good to excellent yield. The method provided advantages; including, excellent yields, recyclability of the catalyst, short reaction times, easy purification and simple procedure.

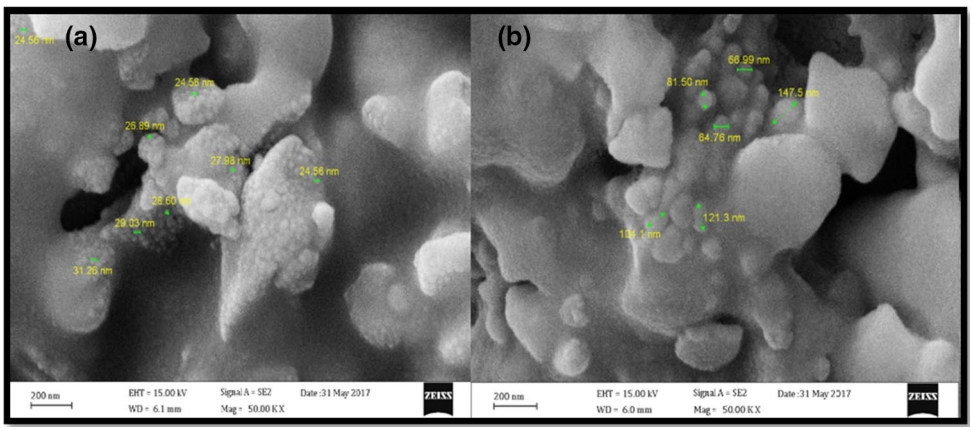

Fig. 3 FE-SEM image of PEA-PSA@CuI **a** before the reaction **b** after the reaction

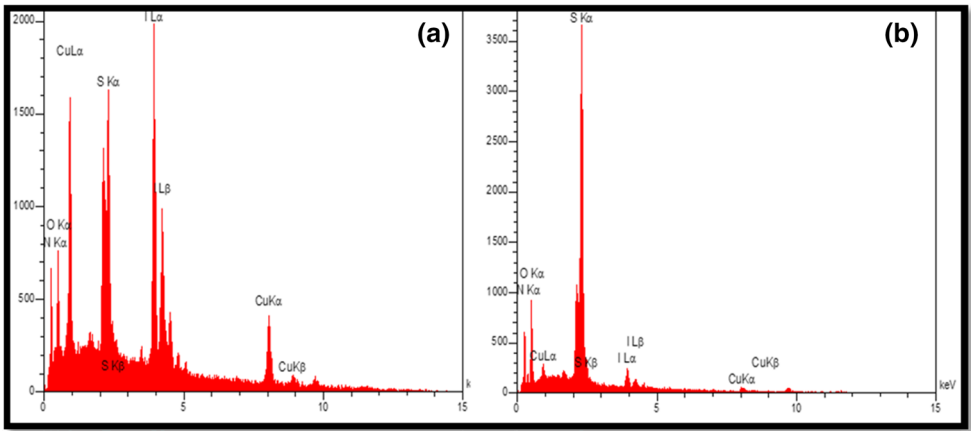

Fig. 4 EDX spectra **a** before the reaction, **b** after the reaction

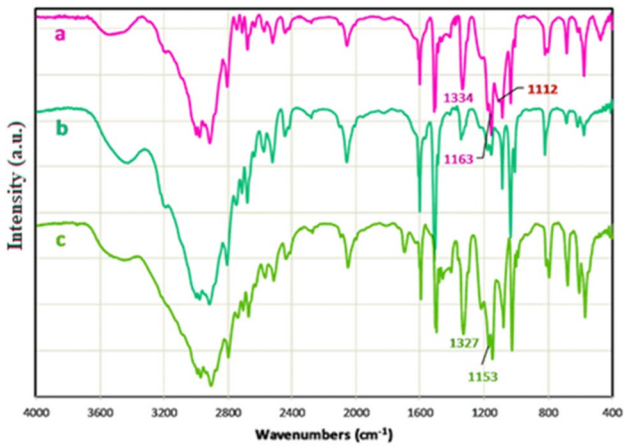

Fig. 5 FT-IR spectra of SiO_2/PEA-PSA (a), porous PEA-PSA (b), and PEA-PSA@CuI (c)

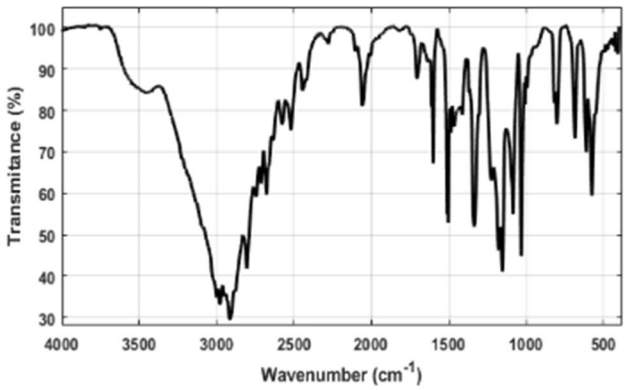

Fig. 6 FT-IR spectra of PEA-PSA@CuI after the reaction

References

1. Ferhat M, Zaoui A, Certier M, Dufour JP, Kgelifa B (1996) Solid-State Mater Adv Technol 30:95
2. Feraoun H, Aourag H, Certier M (2003) Mater Chem Phys 82:597–601
3. Liu Y, Jinhua Z, Jinghui Z, Yitai Q, Kaibing T, Weichao YJ (2001) Mater Sci Lett 20:1865–1870
4. Yang JP, Li P, Wang L (2011) Tetrahedron 67:5543–5549
5. Miao T, Wang L (2007) Tetrahedron Lett 48:95–97
6. Xiao R, Cai R, Yao M (2012) Eur J Org Chem 22:4178–4184
7. Khatri PK, Jain SL (2013) Tetrahedron Lett 54:2740–2743
8. Pazos E, Sleep E, Pérez CMR, Lee SS, Tantakitti F, Stupp SI (2016) J Am Chem Soc 138:5507–5510
9. Gotoh Y, Igarashi R, Nagura M, Ohkoshi Y, Akamatsu K, Deki S (2000) J Mater Chem 10:2548–2554
10. Vaghei RG, Jalili H (2005) Synthesis 7:1099–1102
11. Vaghei RG, Sarmast N (2017) Can J Chem 95:1073–1080
12. Alavinia S, Vaghei RG, Rakhtshah J, Yousefi Seyf J, Arabian IA (2020) Appl Organomet Chem 34:e5449
13. Li B, Gong R, Luo Y, Tan B (2011) Soft Matter 7:10910–10916
14. Yoon J-Y, Lee, Shin H (2011) Curr Org Chem 15:657–674
15. Fustero S, Simón-Fuentes A, Sanz-Cervera JF (2009) Org Prep Proced Int 41:253–330
16. Seung HC, Ji YK, Jaesung K, Sukbok C (2011) Chem Soc Rev 40:4879–4889
17. Bagdi A, Santra KS, Monir K, Hajra A (2015) Chem Commun 51:1555–1575
18. Chernyak N, Gevorgyan V (2010) Angew Chem Int Ed 49:2743–2746
19. Palani T, Park K, Kumar MR, Jung HM, Lee S (2012) Eur J Org Chem 2012:5038–5047
20. Guchhait SK, Chandgude AL, Priyadarshani G (2012) J Org Chem 77:4438–4444
21. Reddy BV, Pathuri SR, Yerabolu JR, Yadav JS (2011) Tetrahedron Lett 52:5789–5793
22. Liu P, Fang L, Lei X, Lin G-Q (2010) Tetrahedron Lett 51:4605
23. Luz I, Xamena FXL, Corma A (2012) J Catal 285:285–291
24. Mishra S, Ghosh R (2011) Synthesis 21:3463–3470
25. Guntreddi T, Allam BK, Singh KN (2012) Synlett 23:2635–2638
26. Chenglong Z, Runsheng Z, Jianping Z (2014) Chem Res Chin Univ 30:632–638
27. Tajbakhsh M, Farhang M, Hosseinzadeh R, Sarrafi Y (2014) RSC Adv 4:23116–23124
28. Mandlimath TR, Sathiyanarayanan KI (2016) RSC Adv 6:3117–3125
29. Hussain N, Gogoi P, Das MR, Sengupta P, Fedorov VE, Asanov IP (2017) Appl Catal A 542:368–379
30. Kharazmi A, Alavinia S (2020) Chem Select 5:1–8
31. Fatehi A, Vaghei RG, Alavinia S, Mahmoodi J (2020) Chem Select 5:944–951
32. Malaekehpoor SM, Derakhshandeh K, Haddadi R, Nourian A, Ghorbani-Vaghei R (2020) Polym Chem. https://doi.org/10.1039/d0py00070a
33. Vaghei RG, Alavinia S, Sarmast N (2018) Appl Organomet Chem 32:e4038
34. Vaghei RG, Alavinia S, Merati Z, Izadkhah V (2018) Appl Organomet Chem 32:e4127
35. Lin J, Huang Hu, Wang Mu, Deng J (2016) Polym Chem 7:1675–1681